Polarized Resonant Inelastic X-Ray Scattering as an Ultrafine Probe of Excited States of La_2CuO_4

Abhay Shukla,[1] Matteo Calandra,[1] Munetaka Taguchi,[2] Akio Kotani,[2,3] György Vankó,[4] and S.-W. Cheong[5]
[1]*Institut de Minéralogie et de Physique des Milieux Condensées, 4 Place Jussieu, 75252, Paris cedex 05, France*
[2]*Soft X-Ray Spectroscopy Lab, RIKEN/SPring-8, 1-1-1, Sayo, Sayo, Hyogo 679-5148, Japan*
[3]*Photon Factory, IMSS, High Energy Accelerator Research Organisation, Tsukuba, Ibaraki 305-0801 Japan*
[4]*European Synchrotron Radiation Facility, BP 220, F-38043 Grenoble cedex, France*
[5]*Department of Physics and Astronomy, Rutgers University, Piscataway, New Jersey 08854, USA*
(Received 6 June 2005; published 24 February 2006)

X-ray absorption is the standard method to probe the unoccupied density of states at a given edge. Here we show that polarized resonant inelastic x-ray scattering in La_2CuO_4 at the Cu K edge is extremely sensitive to the environment of the Cu atom and the fine structure in the Cu $4p$ density of states. Combined *ab initio* and many-body cluster calculations, used for the first time in such a context, show remarkable agreement with experiment. In particular, we identify a nonlocal effect, namely, a transition to *off-site* Cu $3d$ states.

DOI: 10.1103/PhysRevLett.96.077006 PACS numbers: 78.70.Ck, 71.15.Mb, 74.72.Dn, 78.70.Dm

X-ray absorption spectroscopy (XAS) has long been used to investigate the nature of the partial density of excited states at a given absorption threshold. However, preedge features, mainly composed of quadrupolar excitations, are often hard to detect in XAS due to their small intensity and the broadening due to the core-hole lifetime. As a consequence, important insights related to the local environment of the absorbing atom are not readily accessible in XAS. Here we show that resonant inelastic x-ray scattering (RIXS) yields a precise determination of the low-energy unoccupied electronic states in correlated materials. This information is a crucial input for theoretical models seeking to describe excitations in these systems. We study resonant Cu $1s$-$2p$ emission in La_2CuO_4 both from an experimental and theoretical point of view. The excited states in La_2CuO_4 are of interest because of the correlated nature of this compound which on hole doping becomes a high temperature superconductor. The hopping between the Cu $3d_{x^2-y^2}$ and the O $2p_{xy}$ orbitals combined with Coulomb repulsion between Cu $3d$ electrons form the basis for describing the low-energy excitations in this solid [1].

RIXS is a powerful tool for the study of the electronic excitations in solids [2] giving access to site, element, and orbital selective information. It is a second order process where the x-ray emission is measured as the incident x-ray energy is tuned through an absorption edge of the sample. The incident energy determines the intermediate state and the core-hole enhances the cross section [3].

In our experiment in the intermediate state of the resonant process, a $1s$ Cu core electron is excited to states with energies around the preedge region of the Cu K-absorption edge. The final state involves $K\alpha$ emission with filling of the $1s$ hole at the expense of a hole in the $2p$ state. Identifying the measured features and explaining their dependence on incident energy and incident photon polarization is not a trivial task from the theoretical point of view, particularly in strongly correlated systems where single particle theories like standard density functional theory (DFT) dramatically fail due to the lack of important many-body effects. A different approach to the problem is the use of many-body cluster models based on multiband Hubbard-like Hamiltonian. While these methods correctly include many-body effects they often require some knowledge of the empty density of states (DOS) which cannot be easily obtained without the use of *ab initio* electronic structure calculations. For this reason core level spectroscopy is an ideal field for the application of combined *ab initio* and many-body cluster-model approaches.

The orthorhombic structure of La_2CuO_4 with the CuO planes oriented perpendicular to the c axis allows the incident x-ray polarization to be unequivocally defined. Our twinned La_2CuO_4 single crystal was a platelike rectangular sample with the c axis perpendicular to the sample plane and the a/b axis parallel to the sides of the sample (the a/b axes being along the Cu-O bonds). The experiment was performed at beam line ID16 at the European Synchrotron Radiation Facility. The experimental setup was that of a Rowland circle spectrometer with a horizontal scattering plane, using a spherically focusing, bent Si(444) analyzer [4]. The absorption spectrum of La_2CuO_4 was obtained by measuring the total fluorescence yield. We also measured the partial fluorescence yield spectrum by using the spectrometer set to the peak of the $K\alpha_1$ fluorescence line and varying the incident energy as for an absorption measurement. These were measured for two orientations of the sample: in the first geometry (noted a/b) the a-b plane was in the horizontal scattering plane such that it contained both the incident photon momentum and the polarization . They were both oriented at 45° with respect to the a/b axis. Scattering was of the edge of the sample which was about 0.2 mm thick. In the second geometry (noted c) the *a-b* plane, oriented vertically, was perpendicular to the scattering plane. The polarization was at 75° with respect to the *a-b* plane (15° with respect to the *c* axis of the sample). These geometries were also used for the measurement of the $1s2p$ resonant emission. Because of the in-plane polarization of the photons the a/b geometry is sensitive to the in-plane or σ orbitals only while the *c* geometry is sensitive primarily to the π orbitals. The absorption spectrum is characterized by a small prepeak at the onset, usually attributed at least partly to *on-site* Cu $1s$-$3d$ quadrupolar transitions. In Fig. 1 we show the partial fluorescence yield spectra for both geometries. In our RIXS measurements the incident energy is limited to the region around the prepeak (inset of Fig. 1 and left panels of Figs. 2 and 3). It will be seen that the dipolar contribution in this preedge region being small, the weak *on-site* Cu $1s$-$3d$ quadrupolar transition is easily visible. Most importantly we will show that an even weaker *off-site* Cu $1s$-$3d$ dipolar transition mediated by O $2p$ states is also clearly visible in the RIXS spectra. Though the absorption spectrum is relatively featureless, the emission spectra are rich in structure and strongly dependent on the incident energy.

In Figs. 2 and 3 (center) we show the experimental RIXS spectra for incident energies increasing from bottom up. The baseline of each RIXS spectrum corresponds to the incident energy at which it was measured as seen on the partial yield absorption spectrum on the left. RIXS spectra have been arbitrarily shifted such that the lowest energy transfer feature corresponds to the zero of the energy scale and have been normalized to the most intense feature in each spectrum. They show twin features separated by 20 eV due to spin-orbit splitting of the $2p$ core level. In the following we shall discuss only the region from 0 eV to -20 eV energy transfer. The spectra are dominated by a sharp peak at 0 eV which resonates when excitation energies are on the absorption prepeak. In CuO a similar structure has been interpreted as due to a quadrupolar transition [5,6]. By separately calculating the contribution of $1s \rightarrow 3d$ quadrupolar and $1s \rightarrow 4p_\sigma$ and $1s \rightarrow 4p_\pi$ dipolar transitions, we confirm that in La_2CuO_4 this peak is due to the quadrupolar transition. In both geometries two additional features are seen. In the a/b geometry (Fig. 2) a weak, broad peak is observed around -17 eV while a sharp peak at about -3 eV resonates only at higher incident energies. In the *c* geometry (Fig. 3) a strong broad structure with twin peaks at -12 eV and -7 eV is seen while a second peak appears at -5 eV, resonating at higher incident energies. The calculated results of the Cu $K\alpha$ RIXS are shown in Figs. 2 and 3 (right) and are in excellent agreement with the experimental ones. The broad structures at higher energy loss are attributed to virtual transitions due to the main peaks in the Cu $4p$ DOS and are slightly shifted in energy from the measured ones. The lower energy resonant structures are due to transitions to features in the tails of the DOS. These attributions were made by modifying portions of the calculated DOS and tracing the modifications in the calculated RIXS spectrum.

RIXS data are interpreted using a unified *ab initio* and multiplet calculations approach. Numerical multiplet calculations were carried out based on CuO_6^{10-} single cluster model with intra-atomic full multiplets in D_{4h} local symmetry and including the screening channel for charge transfer from O $2p$ ligand state. Only a single Cu atom is retained and charge transfer between the Cu $3d$ state and the neighboring O $2p$ orbitals is allowed. The Hamiltonian is given by $H = H_0 + H_{pd} + H_{dc} + H_{\text{multiplet}}$. H_0 includes the on-site energies of the Cu $1s$ (ε_{1s}), Cu $2p$ (ε_{2p}), Cu $3d$ [$\varepsilon_{3d}(\Gamma)$], Cu $4p$ [$\varepsilon_{4p}(k)$], and Ligand O $2p$ [$\varepsilon_p(\Gamma)$] states; $H_0 = \sum_{\Gamma,\sigma} \varepsilon_{3d}(\Gamma) d^\dagger_{\Gamma\sigma} d_{\Gamma\sigma} + \sum_{m,\sigma} \varepsilon_{2p} p^\dagger_{m\sigma} p_{m\sigma} + \sum_\sigma \varepsilon_{1s} s^\dagger_\sigma s_\sigma + \sum_{k,\sigma} \varepsilon_{4p}(k) P^\dagger_{k\sigma} P_{k\sigma} + \sum_{\Gamma,\sigma} \varepsilon_p(\Gamma) a^\dagger_{\Gamma\sigma} a_{\Gamma\sigma}$.

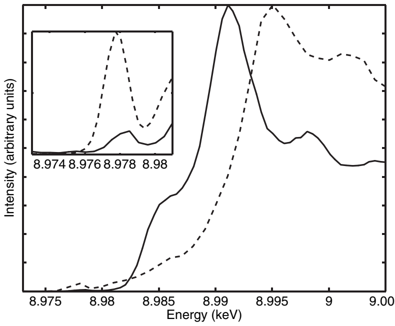

FIG. 1. Partial fluorescence yield absorption spectra for La_2CuO_4 in the *a-b* geometry (dashed line) showing transitions to Cu $4p_\sigma$ orbitals and the *c* geometry (solid line) showing transitions to Cu $4p_\pi$ orbitals. Each spectrum is normalized to its peak. The inset is a zoom of the preedge area where resonant scans are taken.

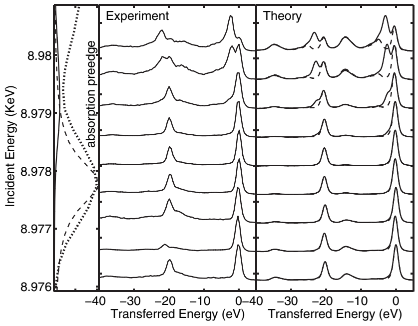

FIG. 2. a/b geometry. Left: the preedge region of the absorption spectrum. Experiment (dotted line), cluster-model calculated *on site* Cu $1s$-$3d$ quadrupolar (dashed line) and *off site* Cu $1s$-$3d$ dipolar contributions (solid line). Center: measured RIXS spectra. The incident energy can be traced to the absorption curve in the left panel. Right: calculated RIXS spectra using *ab initio* Cu $4p$ DOS (solid line) and the modified DOS shown in the inset of Fig. 4 (dashed line). The peak at 0 eV is due to the *on site* Cu $1s$-$3d$ transition. The additional peak appearing at -3 eV in the RIXS spectra is due to the lowest energy feature of the $4p_\sigma$ DOS which is determined by the hybridization with *off site* Cu $3d_{x^2-y^2}$ empty states.

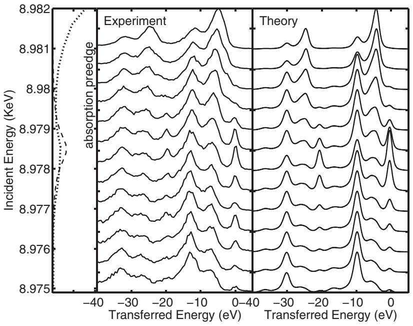

FIG. 3. *c* geometry. Left: the preedge region of the absorption spectrum. Experiment (dotted line), calculated *on site* Cu 1*s*-3*d* quadrupolar contribution (dashed line). Center: measured RIXS spectra. The incident energy can be traced to the absorption curve in the left panel. Right: calculated RIXS spectra.

The irreducible representations of the D_{4h} symmetry are Γ ($= b_{1g}, a_{1g}, b_{2g}$, and e_g). H_{pd} is the hybridization between Cu 3d and O 2p ligand states, $H_{pd} = \sum_{\Gamma,\sigma} V(\Gamma)(d^{\dagger}_{\Gamma\sigma} a_{\Gamma\sigma} + a^{\dagger}_{\Gamma\sigma} d_{\Gamma\sigma})$. The core-hole interaction H_{dc} is composed of two contributions, the attraction between Cu 3d electrons and Cu 1s holes [$U_{dc}(1s)$] and between Cu 3d electrons and Cu 2p holes [$U_{dc}(2p)$], namely $H_{dc} = U_{dc}(1s) \times \sum_{\Gamma,\sigma,\sigma'} d^{\dagger}_{\Gamma\sigma} d_{\Gamma\sigma}(1 - s^{\dagger}_{\sigma'} s_{\sigma'}) + U_{dc}(2p) \sum_{\Gamma,m,\sigma,\sigma'} d^{\dagger}_{\Gamma\sigma} d_{\Gamma\sigma} \times (1 - p^{\dagger}_{m\sigma'} p_{m\sigma'})$. Finally the Hamiltonian $H_{\mathrm{multiplet}}$ describes the intra-atomic multiplet coupling originating from the multipole components of the Coulomb interaction between Cu 3d states and that between Cu 3d and 2p or 1s states and the spin-orbit interactions for Cu 3d and 2p states [7–10].

The parameter values used are (in eV): $U_{dc}(1s) = U_{dc}(2p) = -7.0$, $V(b_{1g}) = 2.5$, $V(a_{1g}) = 1.44$, $V(b_{2g}) = 1.25$, $V(e_g) = 0.88$, $\Delta = 2.75$ (charge transfer energy), $T_{pp} = 1.0$ (hybridization between nearest neighbor O 2p orbitals), very close to the ones used in Ref. [8]. The Slater integrals and the spin-orbit coupling constants are calculated by Cowan's Hartree-Fock program [7] and then the Slater integrals are scaled down to 80%.

The $K\alpha$ RIXS cross section is calculated on the basis of the formula of the coherent second order optical process as $S(\Omega, \omega) = S_D(\Omega, \omega) + S_Q(\Omega, \omega)$ where $S_\alpha(\Omega, \omega)$ with $\alpha = D, Q$ is:

$$S_\alpha(\Omega, \omega) = \sum_f \left| \sum_m \frac{\langle f|T_D|m\rangle\langle m|T_\alpha|g\rangle}{E_g + \Omega - E_m - i\Gamma_K} \right|^2 \times \frac{\Gamma_L/\pi}{(E_g + \Omega - E_f - \omega)^2 + \Gamma_L^2}, \tag{1}$$

and $|g\rangle$, $|m\rangle$, and $|f\rangle$ are the ground, intermediate, and final states of the Hamiltonian H with energies E_g, E_m and E_f, respectively. The incident and emitted photon energies are represented by Ω and ω, respectively. The core-hole lifetime broadening is denoted by $\Gamma_K = 0.4$ eV, half width at half maximum (HWHM) for the 1s core hole and $\Gamma_L = 0.2$ eV (HWHM) for the 2p core hole. Gaussian broadening due to the experimental resolution is taken to be 0.6 eV (HWHM). The operators T_α with $\alpha = D, Q$ represent the optical dipole and quadrupole transition, respectively. The polarization of the incident photon is also taken into account [9,10].

To calculate Eq. (1), we use, as basis states, two configurations, $3d^9$ and $3d^{10}\underline{L}$, where $\underline{L}$ represents a hole in the ligand states. The basis configurations in the intermediate state $|m\rangle$ are $\underline{1s}3d^{10}$ for the quadrupole transition and $\underline{1s}3d^9 4p$ and $\underline{1s}3d^{10}\underline{L}4p$ for the dipole excitation. The final states $|f\rangle$ are $\underline{2p}3d^{10}$ (quadrupole) and $\underline{2p}3d^9 4p$ and $\underline{2p}3d^{10}\underline{L}4p$ (dipole). In the case of dipolar transitions we assume the intermediate states $|m\rangle$ (final states $|f\rangle$) to be a direct product of a Cu 4p state $|k\rangle$ and the remaining system $|m'\rangle$ ($|f'\rangle = |k\rangle|m'\rangle$) with energies $E_m = E_{m'} + \varepsilon_k$ ($E_f = E_{f'} + \varepsilon_k$). Thus we can transform the sum over m in Eq. (1) to a sum over m' plus an integral over the high energy continuum weighted over the 4p Cu projected density of states $\rho_\eta(\epsilon)$ (with $\eta = \sigma, \pi$), namely: $\sum_m \mapsto \sum_{m'} \int d\epsilon \rho_\eta(\epsilon)$ [9].

The Cu 4p projected density of states is calculated *ab initio* [11] using the Kohn-Sham eigenvalues ($\epsilon_{\mathbf{k}n}$) and eigenfunctions ($\psi_{\mathbf{k}n}$) and the orthonormalized atomic orbitals. We disregard the core-hole potential acting on the 4p state, because in this insulating material it is screened strongly by a 3d electron transferred from the O 2p states. In this picture, screening is within the local CuO$_4$ cluster, disregarding an eventual nonlocal screening effect. Since we consider a supercell with two La$_2$CuO$_4$ molecules, ρ_η is also summed over the two inequivalent Cu atoms ($i = 1, 2$). In the *ab initio* simulations we use ultrasoft pseudopotentials [12] with a 45 Ry cutoff and the spin-polarized generalized gradient approximation (SPGGA) [13] for the exchange-correlation kernel. Since using the SPGGA the ground state turns out to be metallic we adopted the SPGGA + U approximation [14] with $U = 8$ eV in the implementation of Ref. [15]. Self-consistence is performed over a $6 \times 6 \times 6$ k-points mesh in the Brillouin zone centered at the Γ point. We converge to an antiferromagnetic state with Cu local magnetic moment $0.625\mu_B$, to be compared with the experimental value of $0.55 \sim 0.60\mu_B$ [16,17]. The band gap is approximately 0.65 eV, in good agreement with previous calculations of Ref. [18] (0.7 eV), but substantially smaller than the one determined from optical conductivity data in Ref. [19] ($\approx$ 2 eV). The Cu $4p_{\sigma,\pi}$ projected DOS calculated on a $N_k = 20 \times 20 \times 20$ k-points mesh are shown in Fig. 4.

For a finer comparison between theory and experiment let us first consider the sharp peak at 0 eV in Figs. 2 and 3 due to the on-site 1s-3d quadrupolar excitations, where the intermediate state is $\underline{1s}3d^{10}$ and the final state is $\underline{2p}3d^{10}$. The $\underline{2p}3d^{10}$ final state shows no multiplet structure because the 3d shell is filled, which explains the single peak

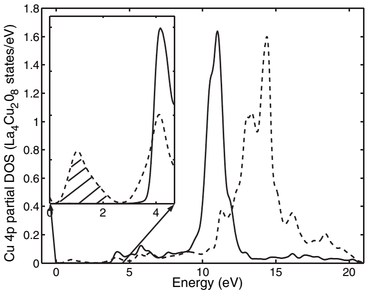

FIG. 4. Projected Cu $4p_\pi$ (solid line) and $4p_\sigma$ (dashed line) orbital density of states calculated *ab initio*. The inset shows the low-energy region in detail. The hatched peak, the lowest energy structure in the Cu $4p_\sigma$ DOS, is induced by hybridization between the Cu $4p_{x,y}$ atomic orbitals, the empty O $2p_{xy}$ orbitals, and the empty $3d_{x^2-y^2}$ orbitals of the neighboring Cu atoms forming a b_{1g} state.

spectral shape. Next, we consider the dipolar contribution. In the a/b geometry the polarization being in the a-b plane, only $1s \rightarrow 4p_\sigma$ transitions contribute. In the c geometry π transitions are visible, the σ component being almost negligible (see Fig. 3). Finally we illustrate the extreme sensitivity of this method by looking for the origin of the peak at -3 eV in the a/b geometry. A closer look at the Cu $4p$ DOS in Fig. 4 reveals that though the main peak of the σ component is at higher energy than that of the π component, the lowest energy structure is σ in nature. The intensity of this structure, peaking at 1 eV, is less than 1% of the total DOS in this region. Nevertheless if this structure is artificially truncated (indicated by the hatching in Fig. 4), the peak at -3 eV disappears in the calculated RIXS (Fig. 2, right, dashed curve). This low-energy structure in the Cu $4p_\sigma$ DOS is induced by the hybridization with O $2p_{xy}$ states and with the Cu $3d$ b_{1g} empty state of the neighboring Cu sites. The small remnant peak at -4 eV in the calculated RIXS using the truncated DOS is due to the tail of pure $4p_\sigma$ character and is much smaller in intensity with respect to the off-site transition for the incident energies in question, confirming our assignment of the -3 eV peak and showing the chemical detail which such a measurement reveals. It is also present in the calculated absorption in the a/b geometry (Fig. 2, left) while absent in the calculated absorption in the c geometry (Fig. 3, left) and in the measured and calculated RIXS (Fig. 3, center and right)

We have conclusively shown with the example of La_2CuO_4 that RIXS at the Cu $K\alpha$ line, together with the unified theoretical approach, provides a sensitive and precise way to determine the Cu $4p$ unoccupied DOS and the interactions of the Cu atom with its immediate environment. In particular, the lowest excitations in La_2CuO_4 include the on-site $1s$-$3d$ quadrupolar transition as well as an off-site $1s$-$3d$ dipolar transition made possible by the surrounding oxygen atoms. We distinguish between the dipolar and quadrupolar part of the transitions and separate them according to their symmetry. We also find that a new approach combining *ab initio* calculations of the partial Cu-$4p$ DOS with many-body cluster calculations is very successful in explaining the data. Indeed both the polarization and incident energy dependence of the spectra are fully explained. Features in the measured spectra are traced to fine details of the calculated Cu-$4p$ DOS giving a sensitive method for checking its reliability and identifying an off-site Cu $1s$-$3d$ dipolar transition. Further perspectives are the definitive attribution of the different features in the Cu K edge x-ray absorption [20,21], as well as investigating the change in excited states as a function of doping [22] and local symmetry (La or Nd based compounds).

M. C. acknowledges discussions with G. A. Sawatzky. This work benefited from CNRS/JSPS research Grant No. 16030. Calculations were performed at the IDRIS supercomputing center (Grant No. 051202). S. W. C. was supported by the NSF-DMR-0405682.

[1] F. C. Zhang and T. M. Rice, Phys. Rev. B **37**, 3759 (1988).
[2] A. Kotani and S. Shin, Rev. Mod. Phys. **73**, 203 (2001); A. Kotani, Eur. Phys. J. B **47**, 3 (2005).
[3] C. C. Kao *et al.*, Phys. Rev. B **54**, 16 361 (1996).
[4] A. Shukla *et al.*, Phys. Rev. B **67**, 081101(R) (2003).
[5] H. Hayashi *et al.*, Phys. Rev. B **66**, 033105 (2002).
[6] G. Doring *et al.*, Phys. Rev. B **70**, 085115 (2004).
[7] R. D. Cowan, *The Theory of Atomic Structure and Spectra* (University of California Press, Berkeley, 1981).
[8] H. Eskes *et al.*, Phys. Rev. B **41**, 288 (1990).
[9] M. Taguchi *et al.*, Phys. Rev. B **61**, 2553 (2000).
[10] H. Shoji *et al.*, J. Phys. Soc. Jpn. **72**, 1560 (2003).
[11] We use the ESPRESSO/PWSCF code, http://www.pwscf.org; S. Baroni *et al.*, Rev. Mod. Phys. **73**, 515 (2001).
[12] D. Vanderbilt, Phys. Rev. B **41**, 7892 (1990).
[13] J. P. Perdew *et al.*, Phys. Rev. Lett. **77**, 3865 (1996).
[14] V. I. Anisimov *et al.*, Phys. Rev. B **44**, 943 (1991); J. Phys. Condens. Matter **9**, 767 (1997).
[15] M. Cococcioni and S. de Gironcoli, Phys. Rev. B **71**, 035105 (2005).
[16] M. T. Czyzyk and G. A. Sawatzky, Phys. Rev. B **49**, 14 211 (1994).
[17] Y. Endoh *et al.*, Phys. Rev. B **37**, 7443 (1988).
[18] I. A. Nekrasov *et al.*, cond-mat/0009107.
[19] S. Uchida *et al.*, Phys. Rev. B **43**, 7942 (1991).
[20] H. Tolentino *et al.*, Phys. Rev. B **45**, 8091 (1992).
[21] N. Kosugi *et al.*, Phys. Rev. B **41**, 131 (1990).
[22] Y.-J. Kim *et al.*, Phys. Rev. B **70**, 094524 (2004).